Opt Quant Electron (2015) 47:99–106
DOI 10.1007/s11082-014-9987-y

FDTD analysis of modal dispersive properties of nonlinear photonic crystal fibers

Tomasz Karpisz · Bartlomiej Salski · Anna Szumska · Mariusz Klimczak · Ryszard Buczynski

Received: 15 January 2014 / Accepted: 5 July 2014 / Published online: 17 July 2014

Abstract This paper presents a full-wave electromagnetic analysis of soft-glass photonic crystal fibers developed for the generation of supercontinuum based on third-order nonlinearity. It is shown that a two-dimensional finite-difference time-domain method for guided problems provides results very similar to the measurement data of real fiber structures, enabling the reduction of costly hardware prototyping, thus, opening the way for the application of FDTD to the modeling of nonlinear optical processes.

Keywords FDTD · Photonic crystal fibers · Supercontinuum · Dispersion

1 Introduction

Photonic crystal fibers (PCFs) are a new class of fibers applicable in areas such as nonlinear optics (Knight and Skryabin 2007), generation of supercontinuum (Dudley et al. 2006), biomedical measurements or sensors (Konorov et al. 2005). Several numerical methods, dedicated to the electromagnetic (EM) analysis of PCFs, have been developed (Szpulak et al. 2006). The most commonly used are the finite element method (Rahman et al. 2007), plane wave expansion method, (Ho et al. 1990), the polar Fourier decomposition method, (Issa and Poladian 2003), finite-difference time-domain (FDTD) method, (Taflove and Hagness

T. Karpisz · B. Salski
Institute of Radioelectronics, Warsaw University of Technology,
Nowowiejska 15/19, 00-665 Warsaw, Poland

B. Salski
e-mail: bsalski@ire.pw.edu.pl

T. Karpisz · M. Klimczak · R. Buczynski
Institute of Electronic Materials Technology, Wolczynska 133, 01-919 Warsaw, Poland

A. Szumska · R. Buczynski (✉)
Faculty of Physics, University of Warsaw, Pasteura 7, 02-093 Warsaw, Poland
e-mail: rbuczyns@igf.fuw.edu.pl

2005), and finite-difference frequency-domain (FDFD) method, (Zhu and Brown 2002). Since dispersive properties of PCFs, critical for nonlinear phenomena, are very sensitive to geometrical properties of a structure, it is essential to have access to a highly reliable EM simulation method in order to reduce costly hardware prototyping to the necessary minimum.

In this paper, a two-dimensional FDTD method developed for guided problems (Gwarek et al. 1993) is applied in a design cycle of PCFs (Salski et al. 2010). The performance of the method is validated against the FDFD method as another widely applicable tool in computational electromagnetics. Both approaches are compared in terms of computational effort and accuracy of obtained results. Eventually, the results are verified against measurement data obtained for microstructured optical fibers (Joannopoulos 2008).

2 Electromagnetic analysis of PCF

PCF with a solid glass core and the cladding composed of a hexagonal air holes lattice is considered (see Fig. 1). Assuming that the geometry of the fiber does not change along a fiber's principal axis, the problem can be reduced to a vector two-dimensional one (V2D), solvable at a plane transverse to the propagation with an analytically imposed longitudinal phase shift (Gwarek et al. 1993):

$$\beta_f = \frac{2\pi}{\lambda_0} n_{eff}, \tag{1}$$

where λ_0 stands for the wavelength in free space and n_{eff} is an effective refractive index of the considered mode.

Consequently, computational effort of the EM analysis can be substantially reduced. In addition, since the analysis is restricted to the fundamental mode with a priori known symmetries, the FDTD model can be reduced to a quarter of the fiber's cross-section with electric and magnetic symmetry conditions imposed, as indicated in Fig. 1. The model is truncated with a perfectly matched layer (PML) surrounding the fiber (Berenger 1996). Before the analysis is started, material properties need to be determined and properly represented with the models available in FDTD. The fibers investigated in this paper are made of Schott glasses, the refractive index of which can be represented by the Sellmeier equation:

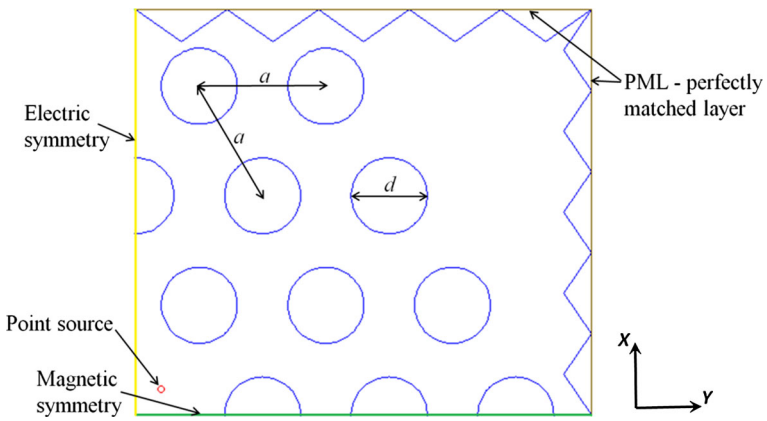

Fig. 1 Quarter of the cross-section of a microstructured fiber, where a is a lattice constant, and d is an air hole diameter

Table 1 Sellmeier and Lorentz coefficients

Model type	Parameters	Glass type	
		TWNN16	PBS517
Sellmeier	B_1	2.496654501	1.5289
	B_2	0.799980033	0.7282
	B_3	1.602289511	0.9981
	C_1	0.016999569	0.0219
	C_2	0.076752705	0.0219
	C_3	149.808796932	100.0000
Lorentz	ε_∞	1.0	1.0
	ε_s	3.4967	2.5289
	f_{p1} (THz)	2,299.3	2,025.8
	f_{p2} (THz)	1,082.1	29.979
	f_{p3} (THz)	24.494	–
	A_1	1.0	1.0
	A_2	0.3204	1.1291
	A_3	0.6418	–

$$n^2(\lambda) = 1 + \frac{B_1\lambda^2}{\lambda^2 - C_1} + \frac{B_2\lambda^2}{\lambda^2 - C_2} + \frac{B_3\lambda^2}{\lambda^2 - C_3}, \tag{2}$$

where n denotes the refractive index of the material, λ is wavelength in microns, $B_{1,2,3}$ and $C_{1,2,3}$ are experimentally determined Sellmeier coefficients.

Since the Sellmeier equation does not have its direct implementation in the FDTD method, a triple-pole Lorentz model is applied instead:

$$\begin{aligned}\varepsilon_r(\omega) = \varepsilon_\infty &+ A_1 \frac{(\varepsilon_s - \varepsilon_\infty)\, 2\pi f_{p1}^2}{2\pi f_{p1}^2 + j\omega 2\pi v_{c1} - \omega^2} \\ &+ A_2 \frac{(\varepsilon_s - \varepsilon_\infty)\, 2\pi f_{p2}^2}{2\pi f_{p2}^2 + j\omega 2\pi v_{c2} - \omega^2} + A_3 \frac{(\varepsilon_s - \varepsilon_\infty)\, 2\pi f_{p3}^2}{2\pi f_{p3}^2 + j\omega 2\pi v_{c3} - \omega^2},\end{aligned} \tag{3}$$

where ε_∞ is optical relative permittivity, ε_S is static relative permittivity, $f_{p1,2,3}$ stand for poles' frequencies, $v_{c1,2,3}$ represents relaxation frequencies, and $A_{1,2,3}$ denote weight coefficients of the corresponding dispersive poles.

As it can be noticed, relaxation frequencies $v_{c1,2,3}$ occurring in the Lorentz model contribute to a non-zero imaginary part of the permittivity model as in (3). It seems to be in contrast with (2), which is purely real. However, according to the Kramers-Kronig theorem (Landau and Lifshitz 1960), frequency dispersion of a real part of a complex function imposes an imaginary part to be non-zero as well. Although imaginary components are neglected in the Sellmeier equations, it is not allowed to do so in FDTD, which explicitly solves Maxwell curl equations in any causal system, such as the one represented with the Lorentz permittivity model as in (3). Otherwise, an FDTD simulation would have become unstable. For those reasons, relaxation frequencies are set non-zero but small enough ($v_{c1,2,3} = 10^{-4} \quad f_{p1,2,3}$) to assure that the loss factor is negligible. Table 1 shows Sellmeier coefficients and the corresponding Lorentz parameters of two glasses, namely TWNN16 and PBS517 (Stępień et al. 2011).

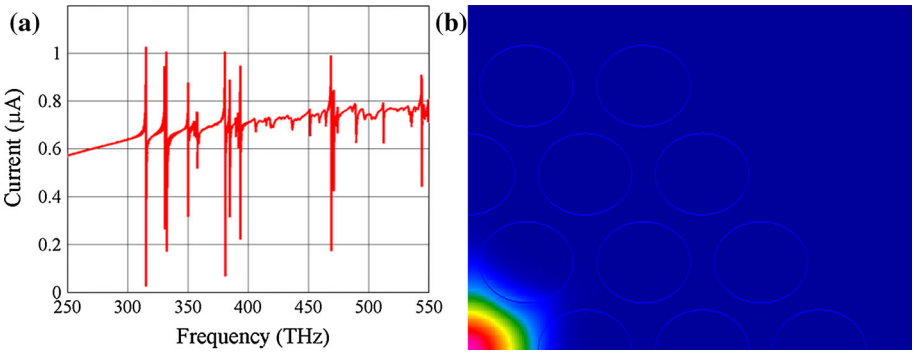

Fig. 2 **a** Spectrum of an injected current ($\beta_f = 21{,}692$ rad/m). **b** Snapshot of an electric field distribution of the fundamental mode occurring at $f = 300$ THz for $\beta_f = 21{,}692$ rad/m

Once the material properties are properly represented, total fiber dispersion can be determined. Total fiber dispersion is comprised of material dispersion and waveguide dispersion. For proper modeling of the fiber both parameters have to be taken into account. Several works previously studied this task (Zhu and Brown 2002; Koshiba and Saitoh 2001; Ferrando et al. 1999).

For total dispersion calculations, several FDTD simulations have to be carried out for a varying longitudinal phase shift β_f as in (1), imposed in the V2D FDTD algorithm. In each simulation run, the structure shown in Fig. 1 is excited with a point source driven with the Kronecker delta to evenly cover the investigated spectrum. Subsequently, the Fourier transform of a current injected by the source, as shown in Fig. 2a, is computed to detect resonances indicating guided modes. Those frequencies (or wavelengths) allow determining effective permittivity n_{eff} of the modes for the imposed β_f imposed in (1). Figure 2b shows an electric field distribution of the fundamental mode occurring at $f = 300$ THz for $\beta_f = 2{,}1692$ rad/m.

Once the spectrum of the effective refractive index n_{eff} is computed, in the subsequent step group velocity dispersion can be computed as:

$$D = \frac{\lambda}{c}\frac{d^2 n_{eff}}{d\lambda^2}. \tag{4}$$

A similar procedure has to be called if the photonic crystal fiber is supposed to be investigated with the FDFD method (Zhu and Brown 2002). A major difference in respect to FDTD is that a single FDFD simulation provides the solution for a single frequency only, so it has to be executed several times, thus, increasing computational effort.

3 Ideal PCF structure

A series of EM simulations for a various set of fiber parameters and types of glasses have been undertaken with both FDTD and FDFD methods implemented in QuickWave and Mode Solutions commercial electromagnetic solvers, respectively. Figures 3 and 4 show calculated characteristics of effective refractive index and dispersion of the fundamental mode propagating in PCFs, which are made of PBS517 and TWNN16 glasses. In both cases, the lattice constant of $a = 1\mu$m is assumed, whereas the filling factor d/a varies from 0.4 to 0.8.

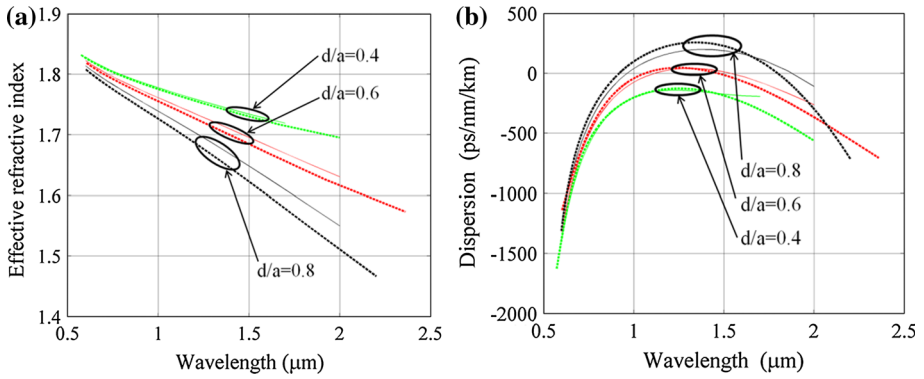

Fig. 3 Effective refractive index (**a**) and dispersion (**b**) of a fundamental mode for the lattice constant of $a = 1\mu$m and the filling factors $d/a = 0.4, 0.6, 0.8$. FDTD (*solid lines*) and FDFD (*dashed lines*) solutions are presented. Lead oxide glass PBS517 is used

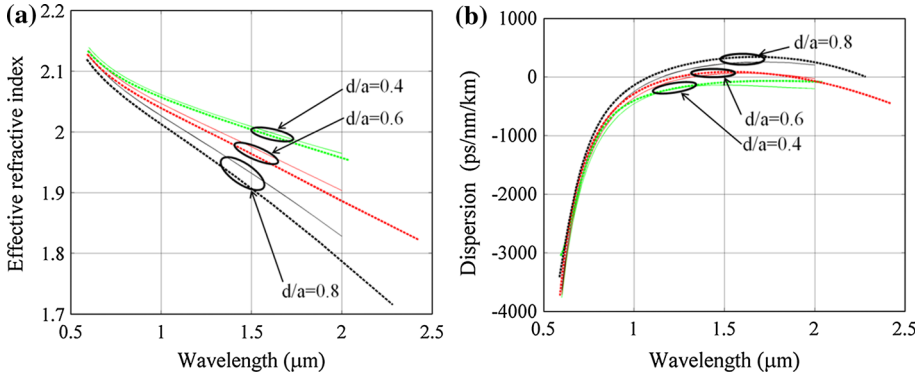

Fig. 4 Effective refractive index (**a**) and dispersion (**b**) of a fundamental mode for the lattice constant of $a = 1.5\mu$m and the filling factors of $d/a = 0.4, 0.6, 0.8$. FDTD (*solid lines*) and FDFD (*dashed lines*) solutions are presented. Tellurite TWNN16 glass is used

Electromagnetic analysis is undertaken on the Intel Core i5-2410M CPU 2.30 GHz platform. Computing time of full range characteristics with FDFD is around 2 h, while in the case of the FDTD model, computation of the whole characteristic takes ca. 1.5 h. It can be noticed that both methods provide very similar results with a regular discrepancy, although FDFD gives slightly lower values of the effective refractive index (see Fig. 3). The discrepancy increases with the filling factor d/a and with the wavelength λ. It can be also noticed that the application of TWNN16 glass results in more flattened dispersion D in the range from $\lambda = 1$ μm up to $\lambda = 2$ μm. However, changing the geometry of the photonic crystal cladding, in terms of the filling factor d/a, allows wider adjustment of the dispersion amplitude in the aforementioned spectrum range, which is essential to the efficient supercontinuum generation (compare Fig. 3b with Fig. 4b).

In the next Section, real PCF geometry will be considered and the corresponding computational results will be validated against measurement data, thus, enabling the validation of the applied EM modeling methods.

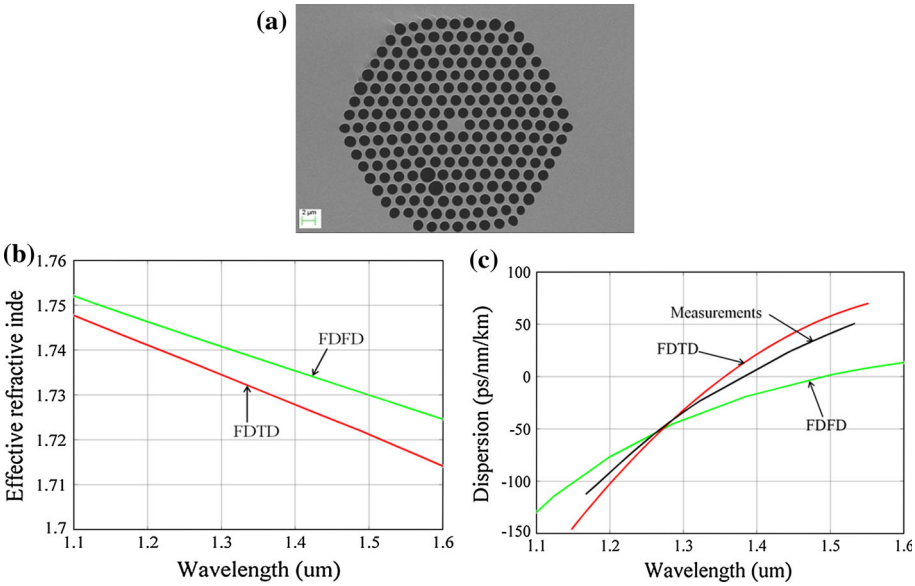

Fig. 5 **a** SEM image of the nonlinear PCF made of lead oxide glass. **b** Effective refractive index of the fundamental mode calculated with FDTD and FDFD methods **c** Dispersion characteristics near ZDW calculated with FDTD and FDFD methods and compared with measurement results

4 Real PCF structure

Photonic crystal fiber is developed using a standard fiber drawing technique available at the Institute of Electronic Materials Technology in Poland (see Fig. 5a). The fiber is made of highly nonlinear lead-bismuth-galate PBG08 glass dedicated for supercontinuum generation (Stepien et al. 2013). Dispersion properties of the fiber are measured with the Mach-Zhender interferometer (Buczynski et al. 2013). The SEM image of the nonlinear PCF has been used as the pattern for the generation of the FDTD and FDFD simulation models.

As it can be seen in Fig. 5c, the measured and calculated dispersion characteristics are in decent agreement, indicating that both numerical methods give reasonable results. However, if the zero dispersion wavelength (ZDW) has to be determined, the FDTD method gives a result much closer to the experimental data. In this case, ZDW is 1,356 and 1,492 nm according to results of the FDTD and FDFD method, respectively, while the measurements indicate that ZDW = 1,382 nm. It means that discrepancy is at the level of about 1.9 and 8.0 % for FDTD and FDFD solutions, respectively. Since determination of ZDW is critical for supercontinuum generation in nonlinear PCFs (Buczynski et al. 2011), the use of the FDFD method can bring a meaningful inaccuracy. Discrepancy between experimental and modeled result is mostly related to credibility of SEM image of the fiber. Since fiber is covers with layer of gold/palladium before the SEM image is taken, diameters of air holes might be slightly different on SEM image and in real fiber. Although the difference is very small it can noticeably influence the dispersion curvature, since dispersion is proportional to the second derivative of effective refractive index (see Eq. 2).

5 Conclusions

Application of the FDTD method to the computation of modal dispersive properties of photonic crystal fibers has been addressed. The accuracy of the proposed method was verified against the FDFD method and against the experimental results. Due to a frequency-domain approach, the extraction of the effective refractive index with FDFD is based on tracing of a selected mode versus wavelength. On the contrary, FDTD allows tracing all the modes simultaneously, which can be advantageous when modes coupling becomes of our interest. In general, both methods give similar results and can be successfully applied to the modeling of photonic crystal fibers.

Acknowledgments This work was supported by the project TEAM/2012-9/1 operated within the Foundation for Polish Science Team Programme co-financed by the European Regional Development Fund, Operational Program Innovative Economy 2007–2013. The authors thank to Dr. R Stepien and D. Pysz from the Institute of Electronic Materials Technology for providing the PCF and Dr. T. Martynkien from Wroclaw University of Technology for the measurement of a dispersion characteristic of the fiber.

References

Berenger, J.P.: Three-dimensional perfectly matched layer for the absorption of electromagnetic waves. J. Comput. Phys. **127**, 363–379 (1996)

Buczynski, R., Pysz, D., Stepien, R., Kasztelanic, R., Kujawa, I., Franczyk, M., Filipkowski, A., Waddie, A.J., Taghizadeh, M.R.: Dispersion management in nonlinear photonic crystal fibres with nanostructured core. J. Eur. Opt. Soc. Rapid Publ. **6**, 11038 (2011)

Buczynski, R., Sobon, G., Sotor, J., Stepniewski, G., Pysz, D., Martynkien, T., Klimczak, M., Kasztelanic, R., Stepien, R., Abramski, K.: Broadband infrared supercontinuum generation in soft-glass photonic crystal fiber pumped with sub-picosecond Er-doped fiber laser mode-locked by graphene saturable absorber. Laser Phys. **23**, 105106 (2013)

Dudley, J.M., Genty, G., Coen, S.: Supercontinuum generation in photonic crystal fiber. Rev. Mod. Phys. **78**, 1135–1184 (2006)

Ferrando, A., Silvestre, E., Miret, J.J., Andres, P., Andres, M.V.: Full-vector analysis of a realistic photonic crystal fiber. Opt. Lett. **24**, 276–278 (1999)

Gwarek, W.K., Morawski, T., Mroczkowski, C.: Application of the FDTD method to the analysis of the circuits described by the two-dimensional vector wave equation. IEEE Trans. Microw. Theory Tech. **41**, 311–316 (1993)

Ho, K.M., Chan, C.T., Soukoulis, C.M.: Existence of a photonic bandgap in periodic dielectric structures. Phys. Rev. Lett. **65**, 3152 (1990)

Issa, N.A., Poladian, L.: Vector wave expansion method for leaky modes of microstructured optical fibers. J. Lightwave Technol. **21**, 1005–1012 (2003)

Joannopoulos, J.D.: Photonic Crystals. Molding the Flow of Light. Princeton University Press, Princeton (2008)

Knight, J.C., Skryabin, D.V.: Nonlinear waveguide optics and photonic crystal fibers. Opt. Express **15**, 15365–15376 (2007)

Konorov, S., Zheltikov, A., Scalora, M.: Photonic-crystal fiber as a multifunctional optical sensor and sample collector. Opt. Express **13**, 3454–3459 (2005)

Koshiba, M., Saitoh, K.: Numerical verification of degeneracy in hexagonal photonic crystal fibers. IEEE Photon. Technol. Lett. **13**, 1313–1315 (2001)

Landau, L.D., Lifshitz, E.M.: Electrodynamics of Continuous Media. Pergamon Press, London (1960)

Rahman, B.M.A., Kejalakshmy, N., Wongcharoen, T., Kabir, A.K.M.S., Grattan, K.T.V.: Full-vectorial solutions of photonic crystal fibers by using the finite element method. In: Proceedings of of Asia-Pacific Microwave Conference (2007)

Salski, B., Celuch, M., Gwarek, W.: FDTD for nanoscale and optical problems. Microw. Mag. **11**, 50–59 (2010)

Stępień, R., Buczyński, R., Pysz, D., Kujawa, I., Mirkowska, M., Diduszko, R.: Development of thermally stable tellurite glasses designed for fabrication of microstructured optical fibers. J. Non-Cryst. Solids **357**, 873–883 (2011)

Stepien, R., Pysz, D., Kujawa, I., Buczynski, R.: Development of silicate and germanate glasses based on lead, bismuth and gallium oxides for midIR microstructured fibers and microoptical elements. Opt. Mater. **35**, 1587–1594 (2013)

Szpulak, M., Urbanczyk, W., Serebryannikov, E., Zheltikov, A., Hochman, A., Leviatan, Y., Kotynski, R., Panajotov, K.: Comparison of different methods for rigorous modeling of photonic crystal fibers. Opt. Express **14**, 5699–5714 (2006)

Taflove, A., Hagness, C.: Photonics. In: Computational Electrodynsmics The Finite-Difference Time-Domain Method, 3rd ed. Artech House (2005)

Zhu, Z., Brown, T.G.: Full-vectorial finite-difference analysis ofmicrostructured optical fibers. Opt. Express **10**, 853–864 (2002)